OPTICAL SECOND HARMONIC GENERATION IN AMMONIUM MALATE

K. BETZLER, H. HESSE and P. LOOSE
Universität, Fachbereich 4, D 45 Osnabrück, Germany

Received 1 April 1977

Second harmonic generation in ammonium malate has been investigated in a wavelength region between 492 nm (short wavelength limit of the harmonic beam at 246 nm) and 640 nm. Phase match angle, refractive indices and all coefficients of the nonlinear susceptibility tensor have been measured; several possibilities for phase matching are discussed.

1. Introduction

Optical second-harmonic generation (SHG) is a well known method to generate intense coherent light in the ultraviolet [1]. Searching new materials usable for phase-matched SHG [2] we investigated the nonlinear optical properties of ammonium malate ($NH_4 \cdot OOC \cdot CHOH \cdot CH_2 \cdot COOH \cdot H_2O$). This salt of the racemic malic acid does not crystallize in monocline prismatic crystals as assumed by several authors [3] but in the monocline domatic structure (point group m resp. C_s) exhibiting only one plane of reflection. Thus most of the quadratic terms of the dielectric polarizability tensor do not vanish. Furthermore, in ammonium malate (AM) the refractive indices are strongly anisotropic. Thus it should allow phase-matched SHG over a wide frequency range.

In the present study we can show for the first time that phase-matched SHG in AM is possible from 246 nm to longer wavelengths. Some phase-match directions have been investigated yielding different long wavelength limits.

From the phase-match (PM) angle measurement, two of the three refractive indices could be determined in the ultraviolet spectral region (the refractive indices in the visible region were measured by a conventional prism method).

Additionally, non-phase-matched SHG measured for several configurations of propagation direction, incident and SH polarization, yielded the possibility of determining all coefficients of the non-linear susceptibility tensor for AM. A comparison to lithium-formate was derived from efficiency measurements.

2. Experimental

The measurements were performed with a flash-lamp pumped dye laser (Chromatix CMX 4) which would be tuned from 480 nm to 640 nm using different dyes (mainly cumarins and rhodamines). The pulse repetition rate was usually 10 Hz; width and power about 1 μs and 10 kW, respectively. The polarization of the laser light could be rotated continuously by rotating a broad-band half-wave retardation plate. The crystals were grown from solution at 35°C and had a typical size of 15 X 15 X 10 mm^3 after cutting and polishing. They could be rotated in the laser beam around a horizontal and a vertical axis, so that all desired crystal directions for the incident polarization could be achieved. The second harmonic beam was detected by a solar-blind photomultiplier with CsTe photocathode (EMI G 26 H 315) after eliminating the fundamental beam by a suitable array of bandpass filters. The laser pulses were monitored via a beam-splitter and a photodiode. Both reference and second harmonic pulses were simultaneously displayed on an oscilloscope. This arrangement served for determining the phase-match angles. For the measurements at low intensities (i.e. in the non-phase-matched configurations) a boxcar-averager

triggered by the photodiode pulses was used as gated integrator in order to improve the signal-to-noise ratio.

3. General

As noticed above, the structure of ammonium malate is C_s. This is one of the lowest symmetries, which is possible in a crystal. In our notation the nonlinear polarizability reads

$$P^i_{NL} = (\chi^i_{jk}) : \vec{E}_j \vec{E}_k \qquad (i,j,k = a,b,c)\,, \tag{1}$$

where the indices j and k refer to the polarization of the incident light. The index i is due to the polarization of the second harmonic. We shall use the common notation, in which the b-axis is perpendicular to the plane of reflection. The a- and c-axis are parallel to the principle optical axes at 500 nm. In the following we shall neglect directional dispersion of the optical axes. This assumption is justified by the experimental results (see below).

From group theoretical considerations, the vanishing components of the nonlinear susceptibility tensor can be determined. Then the nonlinear polarizability is, in the common notation

$$\begin{pmatrix} P^a_{NL} \\ P^b_{NL} \\ P^c_{NL} \end{pmatrix} = \begin{pmatrix} \chi^1_{11} & \chi^1_{22} & \chi^1_{33} & 0 & 2\chi^1_{13} & 0 \\ 0 & 0 & 0 & 2\chi^2_{12} & 0 & 2\chi^2_{23} \\ \chi^3_{11} & \chi^3_{22} & \chi^3_{33} & 0 & 2\chi^3_{13} & 0 \end{pmatrix} \begin{pmatrix} E^2_a \\ E^2_b \\ E^2_c \\ E_a E_b \\ E_a E_c \\ E_b E_c \end{pmatrix} \tag{2}$$

Thus in principle there are ten different χ [4] which are nonzero. The number of coefficients may be reduced to six, if we assume that all indices commute. This is true far away from an electronic transition (Kleinman's-rule) [5].

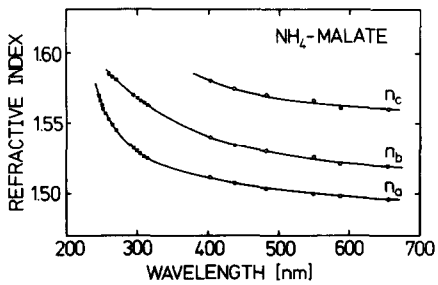

Fig. 1. Refractive indices of ammonium malate. Within the visible region (circles) the refractive indices were measured in the usual way (see text). The squares are due to values, which were computed from the PM-measurements.

Table 1
Possible cases of PM type 1 in crystals with symmetry C_s with $n_a < n_b < n_c$ and normal dispersion

Notation	$E(\omega)\parallel$	$E(2\omega)\parallel$	Observed tensor components
PM 1	c	a.....b	χ^1_{33}
PM 2	b.....c	a	$\chi^1_{22}; \chi^1_{33}$
PM 3	b	a.....c	χ^1_{22}

It is well known from crystal optics [6], that in biaxial crystals the plane of refractive indices $n(\theta, \varphi)$, (θ and φ refer to spherical coordinates with an optical axis as the polar axis) consists of two sheets, n_α and n_β. For normal dispersion $n_{\alpha,\beta}(2\omega)$ is greater than $n_{\alpha,\beta}(\omega)$. If we assume $n_\alpha > n_\beta$, then there are, around each optical axis, only two possibilities for PM

PM type I: $n_\alpha(\omega) = n_\beta(2\omega)$,

PM type II: $\frac{1}{2}[n_\alpha(\omega) + n_\beta(\omega)] = n_\beta(2\omega)$,

where $n(2\omega)$ intersects $n(\omega)$.

In the case of ammonium malate, where $n_a < n_b < n_c$ (see fig. 1), PM type I is possible for the coefficients

χ^1_{22}, χ^1_{33}.

Thus in the case of ammonium malate with symmetry C_s, there exist only the three highly symmetric possibilities for PM type I listed in table 1.

In the visible region, the refractive indices of AM were measured by conventional prism methods (circles in fig. 1).

From these values the possibilities for PM shown in table 1 were derived. Especially the cases PM 1 and PM 2 promised to lead to a small short wavelength limit of PM-SHG because of the large differences between n_c and n_a and n_b, respectively. Therefore we examined these cases in some detail.

4. Results and discussion

For the PM 1 experiments we used a (110)-cut crystal which was rotated around the (001)-direction. Thus

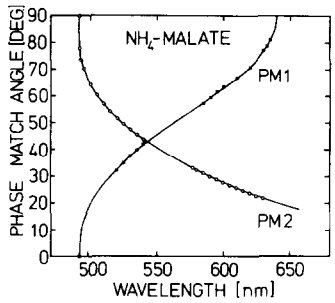

Fig. 2. Phase match angle for PM 1 and PM 2 (compare table 1) as a function of the wavelength of the exciting light. For the definition of the phase match angle see text.

the polarization of the incident radiation could always be chosen parallel to the c-axis. The polarization of the second harmonic is parallel to the a-axis, phase matching is achieved if the condition

$$n_c^2(\omega) = n_a^2(2\omega)\cos^2\theta + n_b^2(2\omega)\sin^2\theta \qquad (3)$$

is satisfied. θ is referred to as the phase match angle and is defined as the angle between the b-axis and the direction of propagation in the a–b plane.

This phase match angle was measured as a function of the wavelength of the incident radiation. The results are shown in fig. 2. It can be seen from fig. 1 and eq. (3) that phase matching in this case is possible only within a certain region of wavelengths. The short wavelength limit of PM1 will be reached if

$$n_c(\omega_s) = n_a(2\omega_s)\,. \qquad (3a)$$

The long wavelength limit of PM 1 is given by the condition

$$n_c(\omega_L) = n_b(2\omega_L)\,. \qquad (3b)$$

In this case however, PM is not possible because for this phase match angle only χ^2_{33} would be excited, which is zero. Thus the corresponding point of the curve PM 1 in fig. 2 is missing. The short wavelength limit for PM 1 is reached at $\lambda_s = 492$ nm. From extrapolation of the curve $\theta = \theta(\lambda)$ the long wavelength limit is found to be $\lambda_L = 640$ nm.

For PM 2 measurement we used (011), (010), and (001) planes of the crystal. The crystal was rotated around the (100) direction. An a-polarized second harmonic was observed. The condition for phase matching in this case is

$$n_a^2(2\omega) = n_b^2(\omega)\cos^2\varphi + n_c^2(\omega)\sin^2\varphi\,. \qquad (4)$$

In this case φ is referred to as the phase match angle within the b–c plane with respect to the c-axis.

The results of these measurements are also shown in fig. 2. The short and the long wavelength limit of PM 2 are determined by the conditions

$$n_a(2\omega_s) = n_c(\omega_s) \qquad (4a)$$

$$n_a(2\omega_L) = n_b(\omega_L)\,. \qquad (4b)$$

Thus the short wavelength limits of PM 2 and PM 1 are coincident. This fact is clearly confirmed experimentally (see fig. 2). Because of normal dispersion, $n_b(\omega)$ is always larger than $n_a(2\omega)$ for $\omega < \omega_s$. Therefore a long wavelength limit of PM 2 does not exist (if IR-absorption can be neglected).

From the knowledge of the refractive indices within the visible region and the PM angle φ for PM 2, the refractive index $n_a(2\omega)$ in the UV-region can be computed according to eq. (4). From $n_a(2\omega)$ and the PM-angle θ for PM 1, $n_b(2\omega)$ was computed according to eq. (3). The results are presented as squares in fig. 1.

In order to understand the different behaviour of n_a and n_b in the UV region, we measured the absorption of ammonium malate. From the fundamental absorption in the IR at 1.44 μm, the crystals are completely transparent throughout the whole visible region. The fundamental absorption in the UV, however, could not be detected with our experimental equipment, which permitted measurements above 180 nm only. However, at 224 nm we detected an absorption band (half-width 44 nm) which we assume to be due to the lowest electronic transition within an OH group (in analogy to the OH^- centres in alkali halide crystals [7]).

The polarization of this absorption band usually is related to the orientation of the OH-axis with respect to the crystallographic axes.

A preferred orientation of certain OH groups may cause the refractive index n_a (and probably n_c) to increase more rapid than n_b near the absorption band at 224 nm.

The measurements of the components χ^i_{jk} of the tensor of the nonlinear dielectric susceptibility were performed at 600 nm. Because of the reasons mentioned above we determined the χ^i_{jk} from non-PM directions. For this purpose we sent the laser light parallel to one principal optical axis of the sample. The incident polarization was rotated continuously by a half-

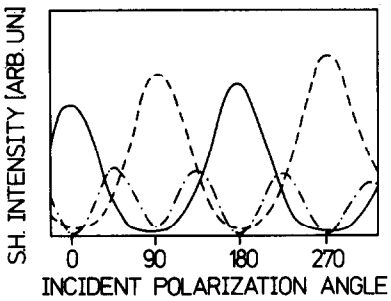

Fig. 3. Polarized SH-intensity as a function of the polarization of the incident radiation. For the solid and the dashed curve the polarization angle is measured about the c-axis. The solid curve is due to the output polarization parallel to c, thus reflects the tensor components χ^3_{33} and χ^3_{11}, whereas the dashed curve was measured with an output polarization parallel to a (tensor components χ^1_{11} and χ^1_{33}). For the dot dashed curve the incident polarization was rotated within the b–c plane ($0° \hat{=} b$, $90° \hat{=} c$), while the output polarization was parallel b (observed tensor component χ^2_{32}).

wave retardation plate. The second harmonic beam was fed through a MgF_2 polarization-prism, which had a fixed polarization direction parallel to a different optical axis, onto the photomultiplier tube. Such an array produces SH-intensity curves $I_i^{SH} = I_i^{SH}(\alpha)$ (with i = SH-polarization), where α is the angle between one of the optical axes and the incident polarization. From the intensities at those angles, where the incident polarization is parallel to one of the optical axes, all tensor-components χ^i_{jk} can be determined. Examples of such curves are plotted in fig. 3.

Consider e.g. the solid curve in fig. 3. The maxima of this curve at $\alpha = 0°$ and $180°$ correspond to the tensor component χ^3_{33}, whereas the minima at $\alpha = 90°$ and $270°$ are due to the coefficient χ^3_{11}. Because only the projection of the incident electric field vector on the c-axis is used to excite the second harmonic, this curve should behave like $\sin^4(\alpha)$ (for $\chi^3_{33} \gg \chi^3_{11}$). Another example is the dot-dashed curve. In this array the output polarization is parallel to the b-axis, and the input polarization is rotated within the a–b plane. Thus the component χ^1_{22} is used for SHG. For the same reasons as above, this curve must behave like $\cos^2(\alpha)$ with maxima half way between the b- and the c-axis. Qualitatively the experimental results confirm these considerations.

From various arrangements it is possible to determine all χ^i_{jk}. However, in some cases the SH-intensities were measured near the PM-condition, in other cases far away from the PM-condition. For this reason it is necessary to correct the measured intensities according to the well known intensity formula [1,8] in order to get the accurate values of the χ^i_{jk}.

$$J^i(2\omega) = J^2_{jk}(\omega)|\chi^i_{jk}|^2 \left(\frac{2\pi}{n(\omega)}\right)^2 \cdot \frac{\sin^2\kappa\,[n(\omega) - n(2\omega)]}{[n(\omega) - n(2\omega)]^2}, \quad (5)$$

$\kappa = \omega l/c = 2\pi l/\lambda$ (l: crystal-length),

$\sin^2(\text{arg.}) \approx \overline{\sin^2(\text{arg.})} = 1/2$ far from PM-conditions.

From these considerations we give the values of χ^i_{jk} in table 2.

Table 2
Relative values of the components of the nonlinear dielectric susceptibility and the experimental arrangements for their observation

Propagation direction	$E(\omega)$	$E(2\omega)$	Observed tensor components	χ^i_{jk}/χ^3_{33} at 600 nm
b	a	a	χ^1_{11}	0.65
	a	c	χ^3_{11}	0.32
	c	a	χ^1_{33}	0.16
	c	c	χ^3_{33}	1.00
c	b	a	χ^1_{22}	0.24
a	b	c	χ^3_{22}	0.21

From various crystallographic arrangements a cross-check of the data in table 2 is possible. Additionally we compared χ^1_{33} with χ^3_{22} of a Li OOCH-crystal [9]. Our result is χ^1_{33} (AM) = 0.21 χ^3_{22} (Li OOCH).

In conclusion, it can be said that ammonium malate is a substance with an UV transmission and a nonlinear susceptibility which can be compared to the corresponding data of Li OOCH. For this reason we are quite sure, that ammonium malate is a useful supplement to the small number of materials, which can be used for PM-SHG in the near UV-region.

References

[1] N. Bloembergen, Nonlinear optics (W.A. Benjamin Inc., New York, Amsterdam 1965).

[2] J.A. Giordmaine, Phys. Rev. Lett. 8 (1962) 19.
[3] L. Pasteuer, Ann. Chim. Phys. (3) 38 (1853) 457;
P. Groth, Chemische Krystallographie, Teil III (Breitkopf und Hartel, Leipzig 1910) p. 301.
[4] M.V. Hobden, J. Appl. Phys. 38 (1967) 4365.
[5] D.A. Kleinmann, Phys. Rev. 126 (1962) 1977.
[6] M. Born and E. Wolf, Principles of optics (Pergamon Press, 1970) p. 665.
[7] S. Kapphan and F. Luty, J. Phys. Chem. Solids 34 (1973) 969.
[8] P.A. Franken, A.E. Hill, C.W. Peters and G. Weinreich, Phys. Rev. Lett. 7 (1961) 118.
[9] S. Singh, W.A. Bonner, J.R. Potopowicz and L.G. van Uitert, Appl. Phys. Lett. 17 (1970) 292.